electronics

MDPI

Communication

Time Jitter Analysis of an Optical Signal Based on Gated On-Off Optical Sampling and Dual-Dirac Modeling

Tao Huang, Zhiqiang Fan *, Jun Su and Qi Qiu *

School of Optoelectronic Science and Engineering, University of Electronic Science and Technology of China, Chengdu 610054, China

* Correspondence: zqfan@uestc.edu.cn (Z.F.); qqiu@uestc.edu.cn (Q.Q.)

Abstract: A time jitter analysis method for an optical signal based on gated on-off optical sampling and dual-Dirac modeling is proposed and demonstrated experimentally. The optical signal under test is firstly sampled by an optical sampling pulse train generated through the gating on-off modulation of a Mach–Zehnder modulator (MZM). The sampled pulse is then broadened using optical true-time delay and electrical low-pass filtering to reduce its bandwidth to match the sample rate of a low-speed electrical analog-to-digital converter (ADC), which is used to quantify the sampled pulse. An eye diagram is obtained from the quantified data and used to plot a time jitter histogram. Finally, the dual-Dirac model is introduced to analyze the time jitter histogram to obtain the total jitter (TJ), including the deterministic jitter (DJ) and random jitter (RJ). In the experiment, a 19.05 ps TJ, including a 13.20 ps DJ and a 5.85 ps RJ, is measured for a 2.5 GHz optical signal using the proposed time jitter analysis method. The results agree well with those measured with a commercial real-time oscilloscope.

Keywords: microwave photonics; time jitter; random jitter; deterministic jitter

Citation: Huang, T.; Fan, Z.; Su, J.; Qiu, Q. Time Jitter Analysis of an Optical Signal Based on Gated On-Off Optical Sampling and Dual-Dirac Modeling. *Electronics* **2023**, *12*, 633. https://doi.org/10.3390/electronics12030633

Academic Editor: Paulo Monteiro

Received: 3 January 2023
Revised: 19 January 2023
Accepted: 24 January 2023
Published: 27 January 2023

1. Introduction

Time jitter, which is generally regarded as the time error when the timing event of a signal deviates from its expected or desirable occurrence time, is one of the main parameters for estimating the performance of digital optical signals and is of fundamental importance for optical communications and cloud computing [1,2]. Conventionally, both asynchronous sampling and synchronous sampling techniques are used to monitor the quality of optical signals [3–6]. In general, timing extraction is necessary for the synchronous sampling-based signal quality monitoring system, whereas asynchronous sampling dispenses with timing extraction. With the explosion of information and the development of round-the-clock information transmission services, online monitoring of optical signal jitter characteristics is of growing importance. Eye diagram analysis, which can be categorized as a synchronous sampling-based time-domain signal monitoring technique, is one of the most popular real-time jitter characterization techniques [5,6]. In general, time jitter analysis using eye diagrams can be broken down into two steps.

The first step is to sample and quantize the optical signal to build an eye diagram. The sampling of the optical signal can be achieved using both electronic [7] and photonic [8–12] techniques. For electrical sampling, the optical signal should be photoelectrically converted to an electrical signal via a wide-band photodetector (PD) and electrically sampled by a high-speed sample-and-hold circuit. However, increasing data rates present implementation challenges for high-speed electronics. One solution is optical sampling, which enables a high temporal resolution for the sampling due to the short optical sampling pulse which can be obtained by a mode-locked laser [8], or nonlinear photonics such as the second-order nonlinear effect [9,10] in nonlinear crystals, or periodically poled $LiNbO_3$ and third-order nonlinear effects [11,12] (Kerr effect) in semiconductor optical amplifiers (SOAs) or optical

fibers. Usually, the generated pulses are as short as around 1 ps, and repetition rates as low as around kilohertz to megahertz. However, it should be noted that although the temporal resolution is increased, the short pulses impose higher quantization efficiency requirements on quantization devices, and the low repetition rates increase the eye diagram formation time. In order to increase the quantization efficiency of low-speed quantization devices and meet the increasing requirements of real-time time jitter monitoring, a delicate balance between temporal resolution and sampling rate is required for the sampling signal. In other words, the sampling pulse generator should have a modest pulse width and repetition rate to accommodate the optical signal data rate. In addition, the repetition rate should be tunable to match optical signals with different data rates.

The second step is to plot the jitter histogram according to the eye diagram to extract the total jitter (TJ), which consists of bounded deterministic jitter (DJ) and unbounded random jitter (RJ) components [13]. Recently, many jitter decomposition techniques [14–17] have been proposed to extract different jitters. For example, Point Net [15], in which the two coordinates of the jitter histogram are used as point cloud data for training, has shown good performance on jitter decomposition. The dual-Dirac model is used to further improve decomposition accuracy [16]. In addition, the dual-Dirac model is also used to assist in improving the accuracy of artificial neural network-based jitter decomposition techniques [17]. It can be concluded that the dual-Dirac model shows an extremely high capability to perform jitter decomposition precisely according to the jitter histogram.

In this paper, a time jitter analysis method that can be carried out in two steps is developed based on gated on-off optical sampling and dual-Dirac modeling. In the first step, the optical signal is sampled through an optical sampling pulse train, and an eye diagram is obtained based on the sampled data. In the second step, a jitter histogram is achieved based on the eye diagram, and the dual-Dirac model is used to implement the time jitter decomposition. The optical sampling pulse train is achieved by the gating on-off modulation of a Mach-Zehnder modulator (MZM). Due to the tunable gigahertz-level repetition rate and tens of ps pulse width of the sampling pulse, the proposed jitter analysis system shows a delicate balance between temporal resolution and sampling rate for a 2.5 GHz optical signal; thus, a real-time jitter analysis can be achieved without using a quantization device with extremely high operation frequency. At the same time, the use of the dual-Dirac model ensures accurate time jitter decomposition. A 21.5 ps TJ, including a 13.2 ps DJ and an 8.3 ps RJ, is measured for a 2.5 GHz optical signal using the proposed time jitter analysis method. The results are verified by a commercial real-time oscilloscope.

2. Theory of Optical Sampling and Time Jitter

Figure 1 shows the schematic diagram of the proposed time jitter analysis method for an optical signal. As can be seen, the jitter analysis can be implemented using two steps. The first step is to obtain an eye diagram using gating on-off optical sampling. The optical signal under test, which can be coupled out from an optical transmission link or source with negligible impact on the signal transmission, is sent to an MZM, where the optical signal is optically sampled by gating on-off sampling pulses from a pulse pattern generator (PPG). In particular, the repetition rate $1/T$ and pulse width $W = 1/(NT)$ of the optical sampling pulse train can be flexibly adjusted by tuning the PPG, where T is the period of the sampling pulse, and N is a positive integer. The sampled optical signal is then transmitted to an optical divider, where the signal is divided into two paths. The two optical signals, which have the same pulse width, repetition rate, and amplitude, are transmitted through two optical fibers with a time delay difference of $\Delta\tau \approx W$ and detected by two photodetectors (PDs). The two detected signals are combined into one path via an electrical coupler (EC) and filtered by a low-pass filter (LPF). Consequently, the sampled pulse is broadened to match the sample rate of a low-speed electrical analog-to-digital converter (ADC), where the broadened sampling pulse is quantified with the same rate as the sampling pulse, and an eye diagram is obtained based on the sampled data. Due to the excellent match between the pulse width of the broadened sampling pulse and the hold

time of the low-speed sample-and-hold circuit, the quantization efficiency of the ADC is improved. In addition, the ADC and the PPG are synchronized through a clock generator to ensure the quantization rate of the ADC matches the sampling rate of the sampling optical pulse train.

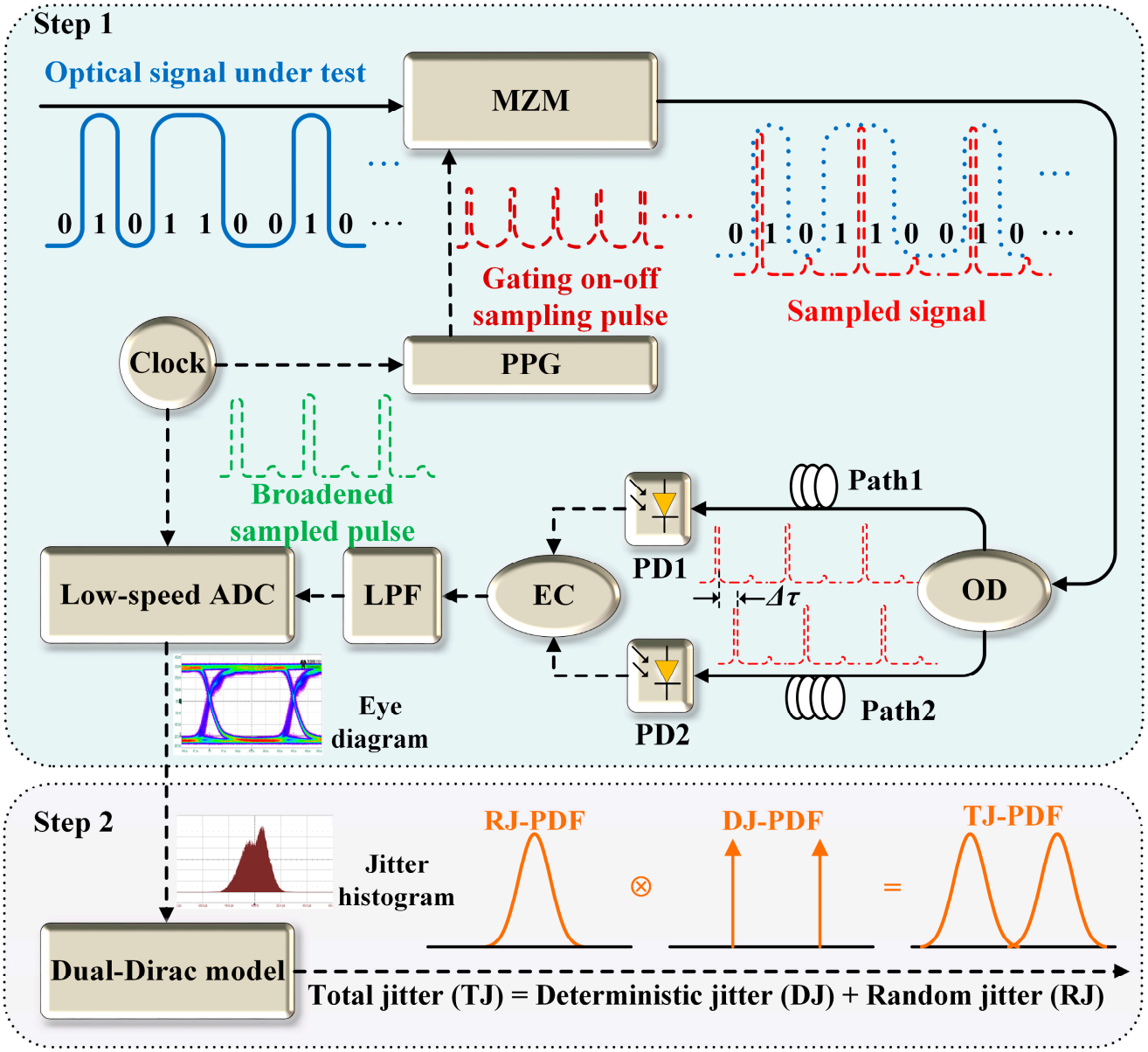

Figure 1. Schematic diagram of the proposed time jitter analysis method for an optical signal. MZM: Mach–Zehnder modulator; OD: optical divider; PD: photodetector; EC: electrical coupler; LPF: low-pass filter; PPG: pulse pattern generator; ADC: analog-to-digital converter; PDF: probability distribution function.

The second step is to implement the time jitter decomposition according to the eye diagram obtained in step 1. Firstly, a time jitter histogram is obtained based on the eye diagram, and a dual-Dirac model [18] is used to realize the jitter decomposition. As shown in Figure 1, the dual-Dirac model is realized based on the statistical-domain jitter probability distribution function (PDF). The TJ-PDF in the dual-Dirac model is the convolution of the RJ-PDF and the DJ-PDF. The TJ-PDF can then be given by [18]

$$\mathrm{PDF}_{TJ}(t) = \mathrm{PDF}_{RJ}(t) \otimes \mathrm{PDF}_{DJ}(t), \quad (1)$$

where t is the time shift relative to the ideal time, and $\mathrm{PDF}_{TJ}(t)$ and $\mathrm{PDF}_{DJ}(t)$ denote the RJ-PDF and DJ-PDF, respectively.

RJ is unbounded in nature and follows a normal or Gaussian distribution. Thus, the RJ-PDF can be described using a normal distribution function as [18]

$$\mathrm{PDF}_{RJ}(t) = \frac{1}{\sqrt{2\pi}\sigma} \exp\left(-\frac{t^2}{2\sigma^2}\right), \tag{2}$$

where σ is the standard deviation of the normal distribution.

DJ is bounded and can be described using two Dirac delta functions as [18]

$$\mathrm{PDF}_{DJ}(t) = \delta(t - \mu_L) + \delta(t - \mu_R), \tag{3}$$

where $\delta(\,)$ is the Dirac delta function, μ_L and μ_R are the deterministic time positions, and the DJ can be presented as $|\,\mu_R - \mu_L\,|$.

According to Equations (2) and (3), Equation (1) is rewritten as [18]

$$\mathrm{PDF}_{TJ}(t) = \frac{\exp\left[-\frac{(t-\mu_L)^2}{2\sigma^2}\right]}{\sqrt{2\pi}\sigma} + \frac{\exp\left[-\frac{(t-\mu_R)^2}{2\sigma^2}\right]}{\sqrt{2\pi}\sigma}, \tag{4}$$

Then the TJ can be given as the sum of the RJ and DJ [18].

$$\mathrm{TJ} = \mathrm{RJ} + \mathrm{DJ}, \tag{5}$$

3. Results and Discussion

A proof-of-concept experiment was carried out based on the setup shown in Figure 1. The optical signal under test with an optical power of 0 dBm was generated from a 2.5 G optical transmitter (CETC-2.5G-SFP). The MZM (CETC-40) has a 3 dB bandwidth of about 40 GHz. Both the PDs (Kang Guan KG-PD-10G) have a 3 dB bandwidth of around 10 GHz and a photoresponsivity of 0.8 A/W. The 3 dB bandwidths of the LPF (Mini-Circuits VLP-41) and EC (Mini-Circuits ZFRSC-123-S+) are 4 and 12 GHz, respectively. The ADC (AcelaMicro) has a maximum sampling rate of 2 Gsps, a 10-bit quantization resolution, and a bandwidth of 4 GHz. A PPG (Anritsu MU183021A) with a 32G-bit/s rate is used to gate the MZM on-off.

Figure 2a shows the measured optical signal (CETC-2.5G-SFP), which was optoelectronically converted through a photodetector and measured by a commercial oscilloscope (Teledyne Lecroy SDA 820Zi-B) with a sampling rate of 80 GS/s, generated from the 2.5 G optical transmitter at a random 20 ns period. It can be seen that the optical signal under test is a random non-return-to-zero (NRZ) code. Figure 2b shows the zoom-in view of the measured optical signal measured from 10.6 to 11.5 ps. As can be seen, the optical signal has a bit time of about 401.5 ps, a rise time of about 140 ps, and a fall time of around 90 ps when the thresholds are 10% and 90% of the amplitude.

The gated on-off sampling performance is evaluated in Figure 3a. The PPG was set to get an electrical pulse train with a frequency of 1.5 GHz and a pulse width of about 83.4 ps, and the electrical pulse train was used to modulate the optical signal injected into the MZM. The optical sampling pulse train plotted by the blue dashed line in Figure 3a was measured using an oscilloscope (SDA 820Zi-B), when a continuous lightwave generated from an optical fiber laser (NKT photonics, Koheras BASIK E15) with an optical power of 0 dBm was injected into the MZM. It can be seen that an optical sampling pulse train with the same period of about 667.0 ps corresponds to a 1.5 GHz sample frequency, and the same pulse of about 83.5 ps as that of the electrical pulse. Replacing the optical fiber laser with a 2.5 G optical transmitter, the sampled optical pulse train after measuring the MZM is shown as the solid red line in Figure 3a. The sampled pulse has the same pulse width of 83.5 ps as that of the electrical pulse.

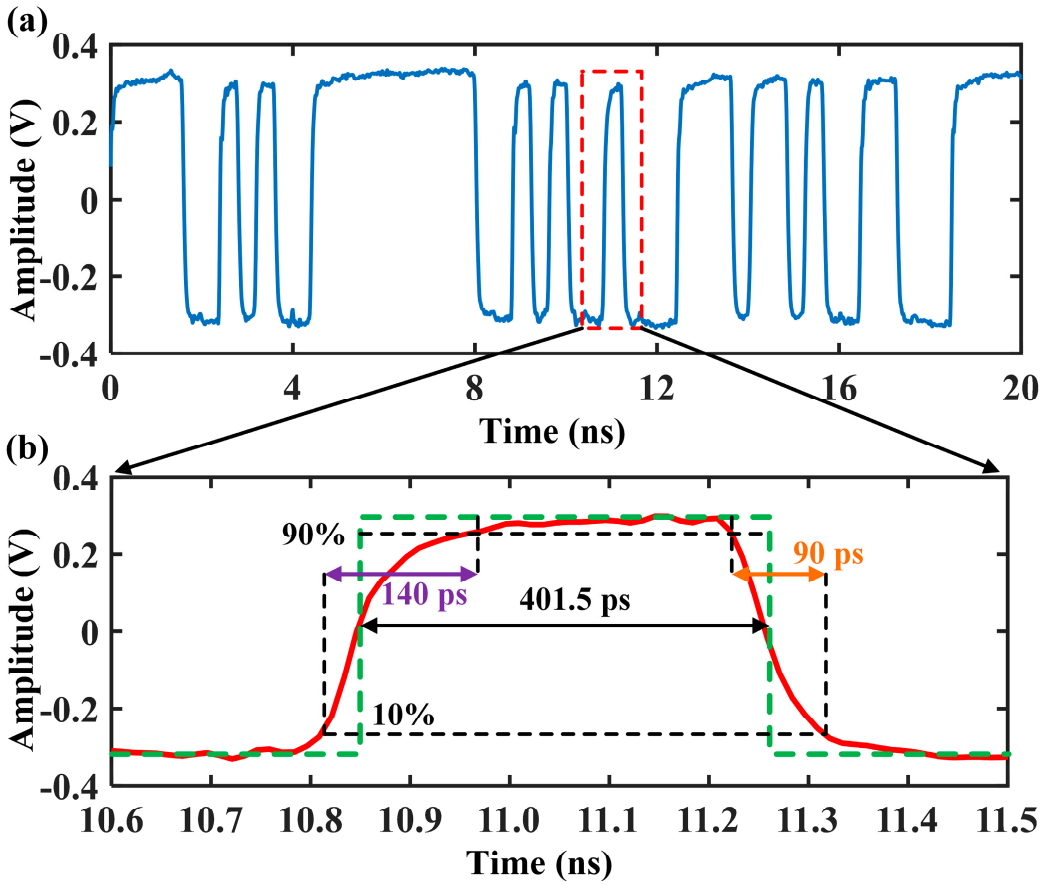

Figure 2. The measured optical signal under test after optoelectronic conversion via a photodetector at (**a**) a random 20 s period, and (**b**) the zoom-in view measured from 10.6 to 11.5 ns.

The sampled optical pulse should then be quantized by the ADC with a maximum sampling rate of 2 Gsps. However, the pulse width of 83.5 ps cannot match the ADC sampling rate, resulting in a low quantization efficiency for the ADC used. To increase the quantization efficiency, the sampled optical pulse is broadened to match the ADC sampling rate. Here, an optical true-time delay technique is used to enlarge the pulse width. Figure 3b shows the measured broadening process of the sampled optical pulse when the input lightwave is generated from an optical fiber laser. The sampled optical pulse is divided into two paths, transmitted through two optical fibers with a time delay difference of about 90 ps, and detected by two PDs. The outputs of the two PDs are plotted as the blue and yellow dashed lines in Figure 3b, where the two pulse trains have a time delay of about 90 ps. The two pulse trains are then combined via an EC and filtered by an LPF with a 3 dB bandwidth of about 4 GHz. The filtered pulse is measured as the solid red line in Figure 3b. It can be seen that the broadened pulse has a pulse width of about 230 ps, which matches the sampling rate of the ADC. Replacing the optical fiber laser with a 2.5 G optical transmitter, the sampled pulse train is plotted in Figure 3c at a random 20 ns period. It can be seen that the sampled optical pulse is broadened, and the pulse width is about 233 ps, which matches the trace-and-hold capability of the ADC. In addition, the sampled pulse has a period of about 667 ps, corresponding to a sampling frequency of 1.5 GHz.

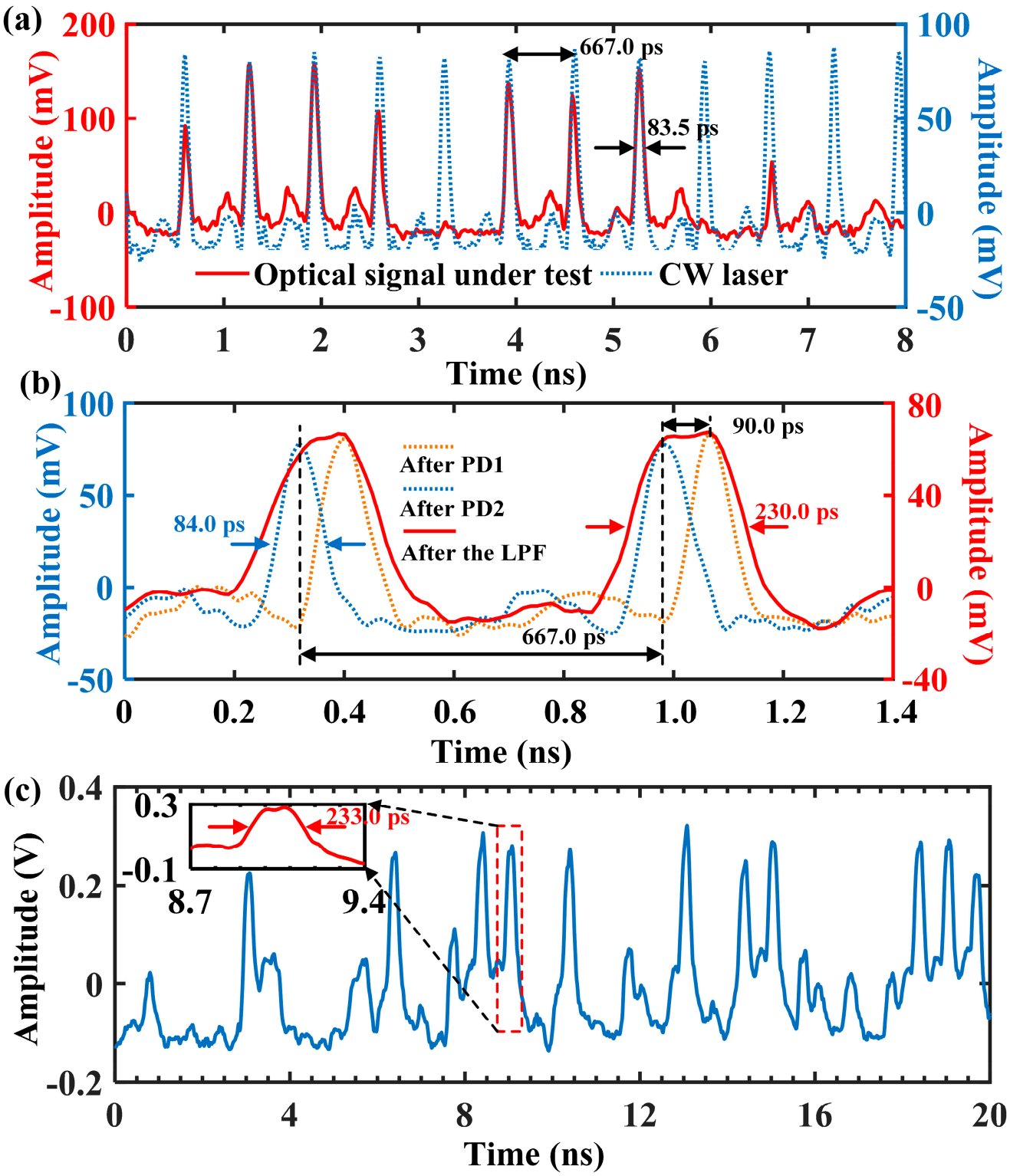

Figure 3. (**a**) The measured optical pulse train after the MZM, and the electrical sampled pulse train after the LPF when the input lightwave of the MZM is from (**b**) a continuous wave laser, or (**c**) a 2.5 G transmitter.

By then synchronizing the PPG and the ADC with a 1.5 GHz clock, the ADC sampling and quantizing time, or the ADC trace-and-hold window, is located at the flat top of the broadened sampled pulse. Consequently, the broadened sampled pulse is quantized by the ADC with high quantization efficiency. The sampling frequency is 1.5 GHz. In

the demonstration, 524,288 points were recorded and used to obtain the eye diagram. Considering the 1.5 GHz sampling frequency, the recording time for the eye diagram is about 350 µs, corresponding to a 2.86 kHz update rate for the eye diagram recording. Figure 4a shows the eye diagram obtained from the quantized data recorded at 524,288 points. The eye width is measured to be about 401.8 ps, which agrees well with the measured 401.5 ps bit time in Figure 2b. The eye diagram measured by the proposed time jitter method is also verified by the eye diagram measured by a commercial oscilloscope (SDA 820Zi-B), as shown in Figure 4b, where the eye width at 401.5 ps is almost the same as that in Figure 4a.

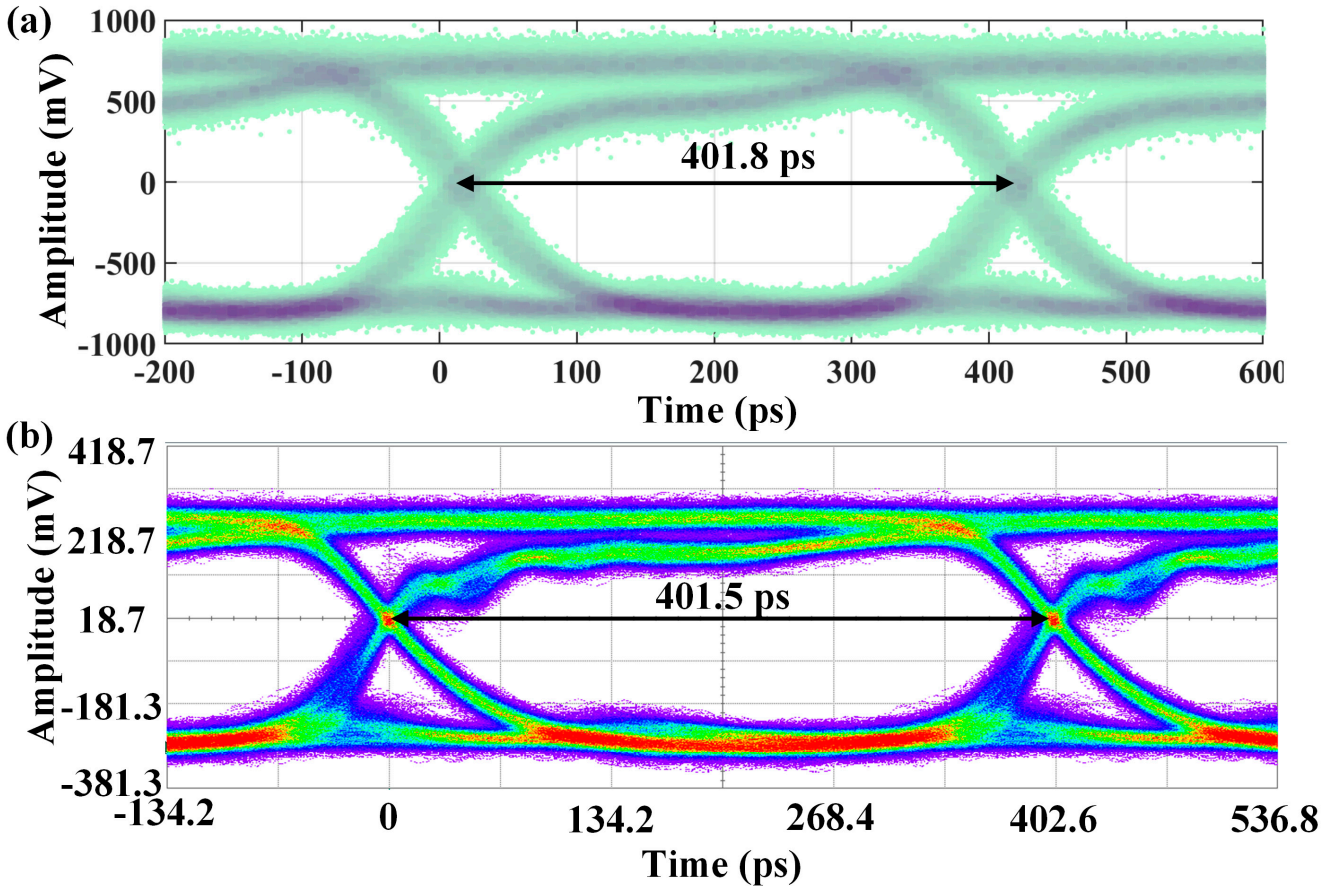

Figure 4. The eye diagrams measured by (**a**) the proposed time jitter analysis method, and (**b**) the commercial oscilloscope SDA 820Zi-B.

The time jitter histogram is then obtained in Figure 5a based on the eye diagram data in Figure 4a. It is shown that the histogram can be viewed as a dual-Dirac distribution. Thus, the jitter decomposition is implemented based on the dual-Dirac model described in Equations (1)–(5). The jitter histogram is fitted as $y = 39.49\ \exp\{-[(t-7.974)/7.378]^2\} + 46.68\ \exp\{-[(t + 5.243)/9.157]^2\}$ with an R-square of 0.9869. The fitting result indicates that the jitter decomposition is implemented through dual-Dirac modeling. Specifically, the deterministic time positions are measured as 7.974 and −5.243 ps, corresponding to a DJ of about 13.20 ps. The standard deviations of the two Gaussian distributions at different deterministic time positions are $7.378/2^{1/2} \approx 5.2$ and $9.157/2^{1/2} \approx 6.5$ ps, corresponding to an RJ of (5.2 + 6.5)/2 = 5.85 ps. The measured TJ is then 13.2 + 5.85 = 19.05 ps. The jitter decomposition results are also verified by those measured by commercial oscilloscope (SDA 820Zi-B) in Figure 5b, where the DJ, RJ, and TJ are measured to be 7.361 + 5.641 ≈ 13.00, $(7.104/2^{1/2} + 9.3/2^{1/2})/2 \approx 5.80$, and 18.80 ps, respectively. It can be seen that the time jitter decomposition results achieved by the proposed jitter analysis method agree well with those of the commercial oscilloscope.

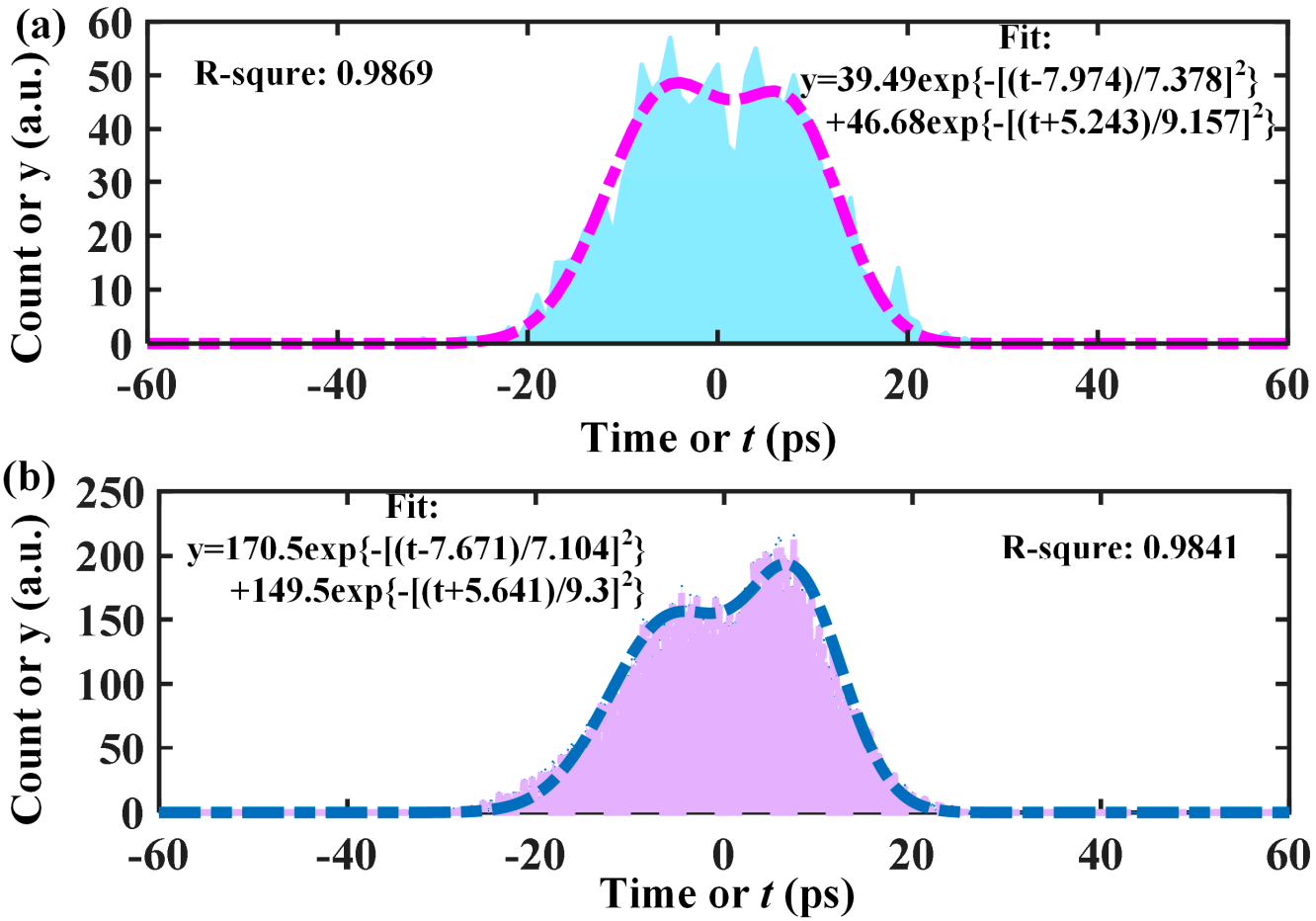

Figure 5. The measured time jitter histograms by (**a**) the proposed time jitter analysis method, and (**b**) the oscilloscope SDA 820Zi-B.

4. Conclusions

In summary, a time jitter analysis method for an optical signal based on gated on-off optical sampling and dual-Dirac modeling was proposed and experimentally demonstrated. The optical signal under test was sampled by an optical sampling pulse train generated through the gating on-off modulation of an MZM. The sampled pulse was then quantized by an electrical ADC, before which the sampled pulse was broadened to increase the quantizing efficiency. According to the quantized data, an eye diagram and a time jitter histogram were obtained. Finally, the time jitter histogram was analyzed using the dual-Dirac model to implement the jitter decomposition. An experimental demonstration was implemented, and a 19.05 ps TJ, including a 13.20 ps DJ and a 5.85 ps RJ, was measured for a 2.5 GHz optical signal. The jitter decomposition results were also verified by the commercial oscilloscope. The successful demonstration of the time jitter analysis method based on optical sampling and dual-Dirac modeling provides a simple and real-time way to realize the time jitter decomposition of an optical signal, which is of fundamental importance for optical communications and cloud computing.

Author Contributions: Conceptualization, Z.F. and Q.Q.; methodology, J.S.; software, T.H.; validation, Z.F., J.S. and Q.Q.; formal analysis, T.H.; investigation, T.H.; resources, Z.F. and Q.Q.; data curation, T.H.; writing—original draft preparation, T.H. and J.S.; writing—review and editing, Z.F. and Q.Q.; supervision, Z.F. and Q.Q.; project administration, Z.F. and Q.Q.; funding acquisition, Z.F. and Q.Q. All authors have read and agreed to the published version of the manuscript.

Funding: This research was funded by the support of the National Natural Science Foundation of China (No. 62201120, No. 61971110), the Research Foundation (No. Y030212059003044), and the National Natural Science Foundation of Sichuan Province.

Institutional Review Board Statement: Not applicable.

Informed Consent Statement: Not applicable.

Data Availability Statement: Data underlying the results presented in this paper are not publicly available at this time but may be obtained from the authors upon reasonable request.

Acknowledgments: The authors would like to acknowledge the support of the National Natural Science Foundation of China, the Research Foundation, and the National Natural Science Foundation of Sichuan Province.

Conflicts of Interest: The authors declare no conflict of interest.

References

1. Dou, Q.; Abraham, J.A. Jitter decomposition in high-speed communication systems. In Proceedings of the 13th European Test Symposium, Verbania, Italy, 25–29 May 2008; pp. 157–162.
2. Bhatheja, K.; Jagannathan, S.; Chen, D. Least Square Based Jitter Decomposition Algorithm for a PAM4 link. In Proceedings of the 2020 IEEE 63rd International Midwest Symposium on Circuits and Systems (MWSCAS), Springfield, MA, USA, 9–12 August 2020; pp. 970–973.
3. Chen, H.; Andrew, W.; Cao, X. Transparent monitoring of rise time using asynchronous amplitude histograms in optical transmission systems. *J. Lightwave Technol.* **2004**, *22*, 1661–1667. [CrossRef]
4. Mrozek, T.; Perlicki, K. Simultaneous monitoring of the values of CD, Crosstalk and OSNR phenomena in the physical layer of the optical network using CNN. *Opt. Quantum Electron.* **2021**, *53*, 640. [CrossRef]
5. Dorrer, C.; Doerr, C.; Kang, I.; Ryf, R.; Leuthold, J.; Winzer, P. Measurement of eye diagrams and constellation diagrams of optical sources using linear optics and waveguide technology. *J. Lightwave Technol.* **2005**, *23*, 178–186.
6. Shake, I.; Takara, H.; Kawanishi, S. Simple measurement of eye diagram and BER using high-speed asynchronous sampling. *J. Lightwave Technol.* **2004**, *22*, 1296–1302. [CrossRef]
7. Jiang, B.; Heiser, D.R. The eye diagram: A new perspective on the project life cycle. *J. Educ. Bus.* **2004**, *80*, 10–16. [CrossRef]
8. Dorrer, C.; Kilper, D.; Stuart, H.; Raybon, G.; Raymer, M. Linear optical sampling. *IEEE Photon. Technol. Lett.* **2003**, *15*, 1746–1748. [CrossRef]
9. Ohta, H.; Nogiwa, S. Measurement of 200 Gbit/s optical eye diagram by optical sampling with gain-switched optical pulse. *Electron. Lett.* **2000**, *36*, 737–739. [CrossRef]
10. Jungerman, R.; Lee, G.; Buccafusca, O.; Kaneko, Y.; Itagaki, N.; Shioda, R. 1-THz bandwidth C-and L-band optical sampling with a bit rate agile timebase. *IEEE Photon. Technol. Lett.* **2002**, *14*, 1148–1150. [CrossRef]
11. Li, J.; Hansryd, J.; Hedekvist, P.O.; Andrekson, P.A.; Knudsen, S.N. 300 Gb/s eye-diagram measurement by optical sampling using fiber based parametric amplification. *IEEE Photon. Technol. Lett.* **2001**, *13*, 987–989.
12. Furukawa, H.; Takakura, H.; Kuroda, K. A novel optical device with wide-bandwidth wavelength conversion and an optical sampling experiment at 200 Gbit/s. *IEEE Trans. Instrum. Meas.* **2001**, *50*, 801–807. [CrossRef]
13. Ren, N.; Fu, Z.; Lei, S.; Liu, H.; Tian, S. Jitter generation model based on timing modulation and cross point calibration for jitter decomposition. *Metrol. Meas. Syst.* **2021**, *28*, 123–143.
14. Ku, C.; Goay, C.; Ahmad, N.; Goh, P. Jitter decomposition of high-speed data signals from jitter histograms with a pole–residue representation using multilayer perceptron neural networks. *IEEE Trans. Electromagn. Compat.* **2019**, *62*, 2227–2237. [CrossRef]
15. Danzer, A.; Griebel, T.; Bach, M.; Dietmayer, K. 2D car detection in radar data with pointnets. In Proceedings of the 2019 IEEE Intelligent Transportation Systems Conference (ITSC), Auckland, New Zealand, 27–30 October 2019; pp. 61–66.
16. Ren, N.; Fu, Z.; Zhou, D.; Kong, D.; Liu, H.; Tian, S. Jitter Decomposition by PointNet-Based Dual-Dirac Model. *IEEE Trans. Electromagn. Compat.* **2022**, *64*, 840–849. [CrossRef]
17. Ren, N.; Fu, Z.; Zhou, D.; Liu, H.; Wu, Z.; Tian, S. Jitter decomposition by convolutional neural networks. *IEEE Trans. Electromagn. Compat.* **2021**, *63*, 1550–1561. [CrossRef]
18. Soliman, G. The accuracy of the Gaussian tail and Dual Dirac model in jitter histogram and probability density functions. *IEEE Trans. Electromagn. Compat.* **2022**, *64*, 2207–2217. [CrossRef]